Lane formation in colloidal mixtures driven by an external field

J. Dzubiella,* G. P. Hoffmann, and H. Löwen
Institut für Theoretische Physik II, Heinrich-Heine-Universität Düsseldorf, Universitätsstraße 1, D-40225 Düsseldorf, Germany
(Received 26 July 2001; published 11 January 2002)

The influence of an external field on a binary colloidal mixture performing Brownian dynamics in a solvent is investigated by nonequilibrium computer simulations and simple theory. In our model, one half of the particles are pushed into the field direction while the other half of them are pulled into the opposite direction. For increasing field strength, we show that the system undergoes a nonequilibrium phase transition from a disordered state to a state characterized by lane formation parallel to the field direction. The lanes are formed by the same kind of particles moving collectively with the field. Lane formation accelerates particle transport parallel to the field direction but suppresses massively transport perpendicular to the field. We further show that lane formation also occurs in a time-dependent oscillatory field. If the frequency of the external field exceeds a critical value, however, the system exhibits a transition back to the disordered state. Our results can be experimentally verified in binary colloidal suspensions exposed to external fields under nonequilibrium conditions.

DOI: 10.1103/PhysRevE.65.021402 PACS number(s): 82.70.Dd, 05.70.Ln, 61.20.Ja, 64.70.Dv

I. INTRODUCTION

While equilibrium bulk phase transitions are by now well understood both by computer simulations [1,2] and by statistical theories [2–4], nonequilibrium situations may induce a much richer scenario of phase transformations. In the last years an emphasis was placed onto such transitions in driven diffusive systems [5–7], which were extensively studied by theory and simulation within lattice and off-lattice models and constant and oscillatory fields [8–10]. In particular, models of identical particles were studied, which couple with a different sign to an external uniform field (so-called ''plus- and minus-charge'' particles) [11]. In the symmetric case where half of the particles are ''plus-charge'' and half of them are ''minus-charge'' particles, a blocking transition was obtained if the field strength exceeded a critical value. The particles then form stripes perpendicular to the field direction [12–14]. This transition has been put forward recently as a concept of panic theory applied to pedestrian zones [15]. Interestingly enough in a two-dimensional off-lattice system confined onto a strip, the blocking transition was found to be generated by increasing the temperature, which is opposite to what one would expect from the equilibrium freezing transition that occurs by lowering the temperature.

In this paper, we focus on another kind of nonequilibrium phase transition in such a driven diffusive off-lattice model with two particle species, which is associated to *lane formation* parallel to the external field. Lanes are formed by bundles of particles of the same kind due to a nonequilibrium ''slipstream'' effect. While such a transition towards lane formation is absent in a square-lattice model with nearest-neighbor hopping and in pure one-component systems, it was recently found in off-lattice simulations of a confined two-dimensional system as an intermediate state between the disordered and the blocked state [15]. In this work, we investigate this lane formation in more detail and map a whole phase diagram as a function of the field strength and the range of the interparticle interaction. In order to characterize the lane phase we use suitable order parameters. We also find an increase of the particle transport in the field direction induced by lane formation and a drastic reduction of particle transport perpendicular to the field direction, which may serve as dynamical criteria for detecting the lane formation. We further show that lane formation is very general and is thus a generic feature of any two-component driven diffusive system. In fact, using computer simulations we demonstrate that lane formation also occurs in unconfined systems, in three spatial dimensions, and for time-dependent oscillatory fields. In the latter case the system exhibits a transition back to the disordered state upon reaching a critical field frequency.

As the occurrence of lane formation appears to be very general, this nonequilibrium transition could be experimentally verified in quite different systems. One evident examples are ionic conductors in an electric field [6]. Another less common example concerns pedestrian (or any other traffic) dynamics where lane formation is an intuitive phenomenon [16]. A further application, which we put forward in this paper, is mesoscopically sized *colloidal suspensions*, which perform diffusive Brownian dynamics in a molecular solvent. Colloidal samples have served as excellent model systems to detect equilibrium phase transitions such as freezing [17] or fluid-fluid phase separation [18]. They have also played a key role for experimental verification of kinetic mode-coupling-type theories describing the (nonequilibrium) kinetic glass transition [19]. Indeed well-characterized colloidal suspensions may also be subjected to external fields resulting in nonequilibrium structure formation. The striking advantage of colloidal samples is that the external field can systematically be controlled and tailored [20]. As possible examples, which realize the Brownian model used in the present study, we mention binary colloids under sedimentation, linear or oscillating shear, and charge-bidisperse colloidal mixtures in electric fields. Another possibility to control colloidal suspensions is by an external laser-optical or mag-

*Email address: joachim@thphy.uni-duesseldorf.de

netic field, which couples to the different dielectric or magnetic permeabilities, respectively, of the solvent and the colloid material. We further mention that two-dimensional systems for which most of the theoretical studies were done can also be realized by squeezing colloids between glass plates [21] or confining them across a water-air interface [22,23] and these can be subjected to external fields as well.

The paper is organized as follows. In Sec. II, we define the model used. Our simulation technique and dynamical properties in the disordered phase where lanes are formed are described in Sec. III. A simple theory is presented in Sec. IV. Section V is devoted to a discussion of the simulation results, in particular, we present nonequilibrium phase diagrams. We conclude in Sec. VI.

II. THE MODEL

In our model, we consider a binary mixture comprising $2N$ Brownian colloidal particles in $d=2$ or $d=3$ spatial dimensions. The particles are either in an area S or in a volume Ω with a fixed total number density of $\rho=2N/S$ and $\rho=2N/\Omega$, respectively. Half of them are particles of type A, the other half is of type B such that the partial number densities are $\rho_A=\rho_B=\rho/2$. The system is held at fixed temperature T being embedded in a bath of microscopic solvent particles of the same temperature. The colloidal particles i and j are interacting via an effective pair potential. For simplicity we study the symmetric case $V_{AA}(r)=V_{AB}(r)=V_{BB}(r)\equiv V(r)$, where r is the interparticle distance. We assume an effective screened Coulomb interaction (or Yukawa form)

$$V(r)=V_0\sigma\exp[-\kappa(r-\sigma)]/r, \tag{1}$$

where V_0 is an energy scale and σ is the particle diameter as a length scale. This is a valid model for charge-stabilized suspensions both in two [24] and three dimensions [17]. The inverse screening length κ governs the range of the interaction and can be tuned, e.g., by the concentration of added salt in the colloidal solution.

The dynamics of the colloids is assumed to be completely overdamped Brownian motion with hydrodynamic interactions neglected, which is a safe approximation if the colloidal volume fraction is small. The friction constant $\gamma=3\pi\eta\sigma$ (with η denoting the shear viscosity of the solvent) is assumed to be the same for both A and B particles. The external constant or oscillatory force acting on the ith particle is pointing in the z direction and modeled as

$$\vec{F}_i(t)=\vec{e}_z f_i P_{\rm rect}(\omega t), \tag{2}$$

where ω is the external frequency (with $\omega\equiv 0$ leading to the constant-field case), $\vec{e}_z$ is the unit vector along the z direction, and f_i is the coupling parameter of the ith particle to the external field. With $P_{\rm rect}(\omega t)$ we apply a rectangular oscillation switching from 1 to -1 defined via

$$P_{\rm rect}(x)=\begin{cases} 1, & n\leqslant x\leqslant (2n+1)/2 \\ -1, & (2n+1)/2<x<n+1 \end{cases} \tag{3}$$

with $n=0\ldots\infty$.

The stochastic Langevin equations for the colloidal trajectories $\vec{r}_i(t)$ $(i=1,\ldots,2N)$ read as

$$\gamma\frac{d\vec{r}_i}{dt}=-\vec{\nabla}_{\vec{r}_i}\sum_{j\neq i}V(|\vec{r}_i-\vec{r}_j|)+\vec{F}_i(t)+\vec{F}_i^{(\rm R)}(t). \tag{4}$$

There are different forces acting onto the colloidal particles: first there is the force attributed to interparticle interactions, then there is the external shaking field and finally the random forces $\vec{F}_i^{(\rm R)}$ describe the kicks of the solvent molecules acting onto the ith colloidal particle. These kicks are Gaussian random numbers with zero mean, $\overline{\vec{F}_i^{(\rm R)}}=0$, and variance

$$\overline{(\vec{F}_i^{(\rm R)})_\alpha(t)(\vec{F}_j^{(\rm R)})_\beta(t')}=2k_BT\gamma\delta_{\alpha\beta}\delta_{ij}\delta(t-t'). \tag{5}$$

The subscripts α and β stand respectively, for the two and three Cartesian components and k_BT is the thermal energy.

In our model we assume the symmetric case $f_i=f^{(\rm A)}\equiv f>0$ for A particles and $f_i=f^{(\rm B)}=-f<0$ for B particles. This is not any restriction. In fact, the asymmetric case $f^{(\rm A)}+f^{(\rm B)}\neq 0$ can directly be mapped onto the symmetric case by subtracting the overall dynamical mode

$$\vec{r}_0(t)=\vec{e}_z\frac{f^{(\rm A)}+f^{(\rm B)}}{2\gamma}\int_0^t P_{\rm rect}(\omega t')dt'. \tag{6}$$

The Langevin equations (4) can be rewritten in terms of new reduced trajectories $\tilde{\vec{r}}_i(t)\equiv\vec{r}_i(t)-\vec{r}_0(t)$ such that the transformed equations have the same form as in the symmetric case with $f=(f^{(\rm A)}-f^{(\rm B)})/2$.

This implies that a binary charged suspension with charges of equal sign is also a good realization of our model: it only matters that the external field acts differently for both species. After a Galilei transformation the symmetric case is realized.

In equilibrium (i.e., in the absence of any external field such that $f=0$) the model reduces to a Brownian Yukawa fluid which has been extensively investigated as far as structural and dynamical equilibrium correlations and freezing transitions are concerned, both in three [25–27] and two [24,28,29] spatial dimensions. Our model is specified by different input parameters such as the total particle density ρ, the thermal energy k_BT, the inverse screening length κ, the dimensionless ratios $U_0=V_0/k_BT$, $f^*=f\sigma/k_BT$, and $\omega\tau_B$, where $\tau_B=\gamma\sigma^2/V_0$ is a suitable Brownian time scale.

III. BROWNIAN DYNAMICS COMPUTER SIMULATIONS IN NONEQUILIBRIUM

A. Simulation procedure

Our Brownian dynamics code is similar to earlier nonequilibrium simulations of charge-polydisperse colloids [30–32]. For $d=2$, we put $N=250\,A$ and $N=250\,B$ particles into a square cell of length ℓ with periodic boundary conditions. The total colloidal number density is $\rho=2N/\ell^2$. Likewise, in three dimensions, $N=500$ A and B particles are in a cubic box of length ℓ such that $\rho=2N/\ell^3$. For the snapshots of

the $d=3$ system (Fig. 3) we increased the number to $2N=8000$ particles for a better resolution of the structure. We checked that the results are not dependent of the number of simulated particles; except for small numbers, we found the usual finite-size effects. The direction of the external force is always along an edge of the simulation cell.

We tried different starting configurations. The system was observed to run into a non-equilibrium steady-state independent of the initial configuration.

The Langevin equations of motion including the shaking external field were numerically solved using a finite time step Δt and the technique of Ermak [1,33]. The typical size of the time step was $\Delta t=0.003\tau_B$. We simulated typically 2×10^4 time steps, which corresponds to a simulation time of $60\tau_B$. After an initial relaxation period of $20\tau_B$, statistics were gathered.

B. Order parameter

In order to detect the transition towards lane formation a sensitive order parameter is needed. A suitable order parameter could probe particle density inhomogeneities along the field in the z direction, which vanish in an ideal lane configuration. Therefore, we assign to every particle i an order parameter ϕ_i, which is chosen to be 1, when the lateral distance $r_1=|x_i-x_j|$ ($r_1=\sqrt{(x_i-x_j)^2+(y_i-y_j)^2}$ in three dimensions) to all particles j of the other type is larger than a suitable length scale, say $r_1>\rho^{-1/d}/2$. Otherwise, ϕ_i is set to zero. A global dimensionless order parameter ϕ can now be defined as

$$\phi=\frac{1}{N}\left\langle \sum_{i=1}^{N} \phi_i \right\rangle, \tag{7}$$

where the brackets denote a time average. In a completely mixed state, ϕ vanishes while for ideal AB separation, $\phi=1$.

A typical result for ϕ as a function of field strength f is shown for $d=2$ and a constant field ($\omega=0$) in Fig. 1. While ϕ is small for a small constant field, it grows when a critical field strength f_c is approached. Further increasing of the external field yields values close to unity. The transition towards lane formation is reversible but exhibits a significant hysteresis. This can be deduced from Fig. 1(b) where the external field strength was slowly decreased. Hence we conclude that lane formation is a nonequilibrium first-order transition. As can be deduced from Fig. 1, the critical field strength f_c increases with increasing κ. More results for the location of the nonequilibrium phase transition will be presented in Sec. V A.

Simulation snapshots associated with a situation without a field as well as with a field below and above the critical field strength are shown in Figs. 2(a)–2(c). One clearly sees lane formation parallel to the external field. A further characteristic length scale corresponding to lane formation is the averaged thickness of the lanes. In the snapshots, this thickness of the lanes is about several interparticle spacings. It may be conjectured, however, in analogy with lattice models [6] that the finite width of the lanes is due to a lack of relaxation into the final steady state, which is a fully phase-separated situation.

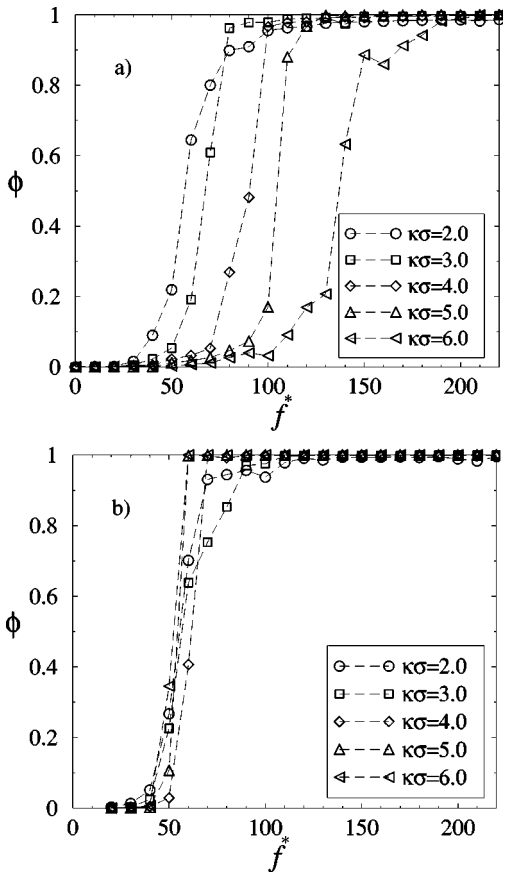

FIG. 1. Dimensionless order parameter ϕ as a function of field strength f^* for $d=2$ and different inverse screening lengths $\kappa\sigma$. In (a) the field is increased starting from a randomly mixed configuration, while in (b) the initial configuration is completely demixed (two lanes) and the field is decreased. The density is $\rho\sigma^2=1.0$ and $U_0=2.5$, $\omega=0$.

We have, furthermore, considered situations with nonvanishing field frequencies ω. If an oscillatory field with amplitude $f>f_c$ is present and the frequency ω is increased, the order parameter ϕ decreases with increasing ω. For low frequencies the system remains in the lane state, $\phi\approx1$, while above a critical frequency, the system gets back to disorder and ϕ fades to zero.

All these considerations are the same for a three-dimensional system. Corresponding snapshots with lane configurations are shown in Figs. 3(a) and 3(b). Of course, due to the presence of an additional dimension, the lane structure is more complicated in three dimensions (3D) than in 2D. A cut through a plane perpendicular to the field is shown in Fig. 3(b) demonstrating that the in-plane structure is reminiscent of a two-dimensional phase separation or a percolating network.

C. Dynamical diagnostics

For a constant field ($\omega=0$), we have also computed a dynamical correlation in the nonequilibrium steady state fo-

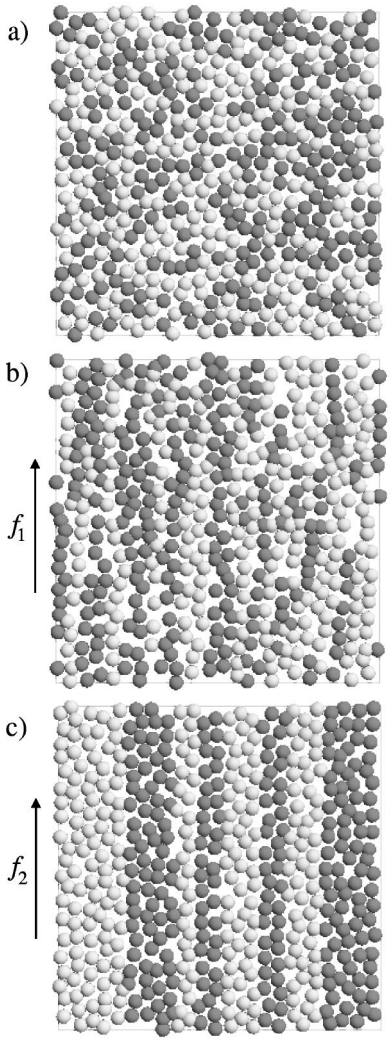

FIG. 2. Typical simulation snapshots of the two-dimensional system: (a) disordered state without field ($\phi=0$), (b) disordered state with field $f_1 \approx f_c$ ($\phi \approx 0.45$), (c) lane formation with field $f_2 > f_1$ ($\phi \approx 0.99$). The particles are depicted as spheres with diameter σ. A light sphere is an *A* particle while a gray sphere is a *B* particle. The parameters are $\kappa\sigma=4.0$, $\rho\sigma^2=1.0$, $U_0=2.5$, and $\omega=0$.

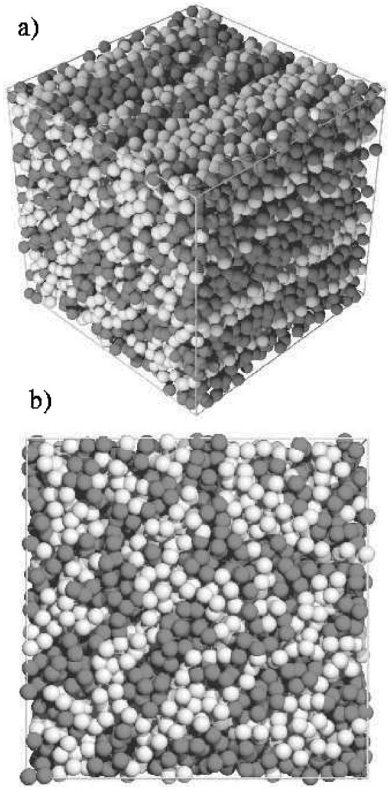

FIG. 3. Typical snapshots of the three-dimensional system with external field $f>f_c$ and lanes parallel to the field: (a) three-dimensional view, (b) look on the (x,y) plane perpendicular to the field direction z. The particles are rendered as spheres with diameter σ. For these snapshots we simulated $2N=8000$ particles. The parameters are $\kappa\sigma=2.0$, $U_0=2.5$, $\rho\sigma^3=1.0$, and $\omega=0$.

cusing on particle transport properties parallel and perpendicular to the external field. In fact, as expected, the particle transport in field direction is enhanced once lanes have been formed. In detail, for a constant field, we define the averaged drift velocity v_D along the field for each particle species by measuring the mean-square displacement in the z direction in the nonequilibrium steady state by

$$v_D^2 := \lim_{t\to\infty} \frac{\langle [(\vec{r}_i(t)-\vec{r}_i(0))\cdot\vec{e}_z]^2\rangle}{t^2} \tag{8}$$

Clearly, as the long-time dynamics is diffusive in equilibrium, $v_D=0$ for $f=0$. In the mixed state v_D is small as the external field enforces a transport, which is, however, still hindered by the presence of different particle species. Once lanes are formed, v_D increases as the obstacles made up by different particle species are not any longer present signaling an efficient particle transport along the lanes in directions parallel to the field. An example of v_D versus increasing field strength f for $d=2$ is shown in Fig. 4(a). These results are compared to the drift velocity of a one-component Brownian system in an external field, where

$$v_D \equiv v_0 = f/\gamma, \tag{9}$$

corresponding to a trivial overall dynamical mode of all the particles. Indeed during lane formation, as probed by the order parameter ϕ, the drift velocity practically equals v_0. For small fields, on the other hand, v_D is significantly smaller than v_0. Hence lane formation manifests itself in a dynamical anomaly in the drift velocity, which can be used as a dynamical diagnostics to detect lane formation.

A more dramatic effect is observed for the long-time diffusion coefficient perpendicular to the field direction as defined via

$$D_L := \lim_{t\to\infty} \frac{\langle [(\vec{r}_i(t)-\vec{r}_i(0))\cdot\vec{e}_x]^2\rangle}{2t}. \tag{10}$$

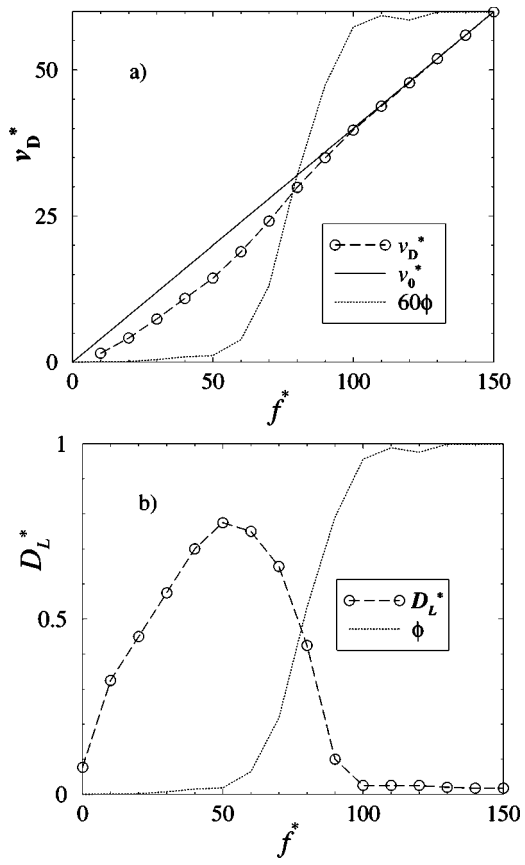

FIG. 4. (a) Averaged dimensionless drift velocity $v_D^*=v_D\tau_B/\sigma$ in z direction versus the external field f^* compared to the dimensionless drift velocity $v_0^*=v_0\tau_B/\sigma$ of a one-component Brownian system and to the order parameter ϕ. (b) Dimensionless long-time diffusion coefficient $D_L^*=D_L\tau_B/\sigma^2$ in x direction versus f^* also compared to ϕ. In (a) the ϕ curve is inflated to the maximal shown ordinate value for better comparison. The parameters are $d=2$, $\kappa\sigma=4.0$, $U_0=2.5$, $\rho\sigma^2=1.0$, and $\omega=0$.

For a vanishing external field in equilibrium, the long-time self-diffusion coefficient D_L has been the subject of intense recent research, in particular, for Brownian-Yukawa systems as studied here [34–41]. Turning on the external field strength f, particles of different types can only follow the external field by eluding each other, so that the diffusion perpendicular to the external field has to increase with f. This effect grows until the critical field strength is reached and the system begins to form lanes. Now the particles are confined to lanes with thickness of some interparticle spacings, which reduces the perpendicular diffusion again. Results for D_L versus f are shown in Fig. 4(b) for $d=2$, together with the corresponding order parameter ϕ, and confirm these qualitative considerations. The drastic decrease of D_L versus f strongly correlates with the location of the lane formation as indicated by a strongly increasing parameter ϕ. This drastic decrease can be exploited as a sensitive dynamical diagnostics to locate lane formation. We remark that after a very long time, lanes may fuse towards big nonstructured regions. In this case, the final falloff of D_L for $f>f_c$ can be slightly shifted upwards to the equilibrium diffusion coefficient at $f=0$.

IV. SIMPLE THEORY

A. Constant field

We are aiming at a rough theoretical estimation of the boundaries of the laning transition with constant external field f in two or three dimensions. We assume that the system goes into the stratified state when the external field is larger than the typical average force between two particles of opposite type. The latter depends both on density and on the external field itself. We estimate a typical average force between two opposite particles by considering different ''effective'' interparticle spacings. The first typical interparticle spacing is set by the density alone, $a=\rho^{-1/d}$. Including fluctuations in the interparticle distance induced by a finite temperature results in a further smaller effective average distance $\tilde{a}$ as obtained by setting a typical interparticle energy equal to $V(a)+k_BT$. Hence $\tilde{a}=V^{-1}[V(a)+k_BT]$ where V^{-1} is the inverse function of the interaction potential $V(r)$. Finally the presence of an external field enforces an even smaller averaged distance a' between colliding opposite particles, which can be estimated via

$$a'=F^{-1}[f+F(\tilde{a})], \tag{11}$$

where F^{-1} is the inverse function of $F(r)=-\nabla V(r)$. In general, a pair of opposite particles will not collide centrally such that the actual average distance is between a' and $\tilde{a}$. Hence the averaged force $\overline{f}$ between an A and a B particle is roughly

$$\overline{f}=\frac{1}{\tilde{a}-a'}[V(a')-V(\tilde{a})]. \tag{12}$$

The critical force f_c is reached when the external force becomes of the order of the mean force $\overline{f}$,

$$f_c=\alpha\overline{f}. \tag{13}$$

α is a yet not known dimensionless prefactor of the order of unity, which should depend, in general, on the dimensionality d. It will be determined later by an optimal fit with our simulation results, see Sec. V A.

B. Oscillatory field

We now focus on a time-dependent external field (2) with nonvanishing frequency. We propose a simple theory that predicts the critical frequency $\omega\equiv\omega_c$ upon which a transition back to the disordered state occurs. Let the field amplitude f be such that $f>f_c$ holds. In the segregated mixture the particles are moving collectively with the external field. Their velocity in field direction changes sign but roughly has the modulus of the drift velocity v_0, Eq. (9). At the interfaces between two lanes, there is an additional friction due to the opposite moving particles of the other type. This additional friction should scale with the range $1/\kappa$ of the interparticle interaction in terms of a typical microscopic spacing σ. Hence the drift velocity v_I near an interface is

$$v_1 \approx \frac{f}{\gamma[1+1/(\kappa\sigma)]}, \tag{14}$$

which changes, however, its sign periodically according to the shaking external field. Now we consider the stability of two lanes at their interface. The field frequency has to be small enough in order to provide a sufficiently long time period in which the two lanes can slide against each other avoiding a mixing of different particle species. If this time is getting very small, diffusion perpendicular to the field direction will dominate and destroy the sharp interface. Lane stability is lost when a particle has roughly reached a typical interparticle spacing $a=\rho^{-1/d}$ during half a period $1/2\omega$ of the external field. Thermal fluctuations can be neglected compared to the high critical force. This yields for the critical frequency

$$v_1/2\omega_c \approx \rho^{-1/d} \tag{15}$$

or

$$\omega_c \approx \frac{f\rho^{1/d}}{2\gamma[1+1/(\kappa\sigma)]}. \tag{16}$$

This result can be understood both in a more qualitative and more quantitative way. Qualitatively, it can be interpreted as a scaling law predicting different exponents for the transition frequency for varying field strength, friction coefficient, screening length, and particle density. Note that in our theory the transition frequencies are independent of temperature. Furthermore, Eq. (16) is a full quantitative prediction, which we shall test against our computer simulation data in Sec. V B.

V. RESULTS FOR THE NONEQUILIBRIUM PHASE DIAGRAM

A. Constant field

The phase diagram for a constant ($\omega=0$) external force obtained from computer simulations is shown in Fig. 5(a). The location of the phase transition is estimated via the behavior of the order parameter ϕ: the critical field strength f_c^* is obtained by setting $\phi=0.5$ for a set of runs with increasing field strengths f^*. The plots clearly show that for increasing density ρ or increasing interaction energy U_0, an enhanced critical force f_c is necessary to drive a transition towards lane formation. By increasing one of these two parameters the correlation between the particles is getting stronger, so as a conclusive result we can state that whenever the correlation is increased the critical force is getting higher. A bit more subtle is the dependence on κ, which is the inverse range of the interaction potential and controls the ''softness'' of the interaction. By watching, e.g., the pair correlation function in equilibrium, one observes an increase in correlation for increasing κ. This explains why the critical field strength f_c^* is increasing with κ, although this increase is practically marginal for small densities. We also remark that, for densities $\rho\sigma^2=1.0$ or $\rho\sigma^3=1.0$ in three dimensions and high $\kappa\sigma \approx 5,6$, the system is slightly below the equilibrium bulk freezing transition [25,29]. The particles are highly correlated and the external force has to be strongly enhanced to enforce stratification.

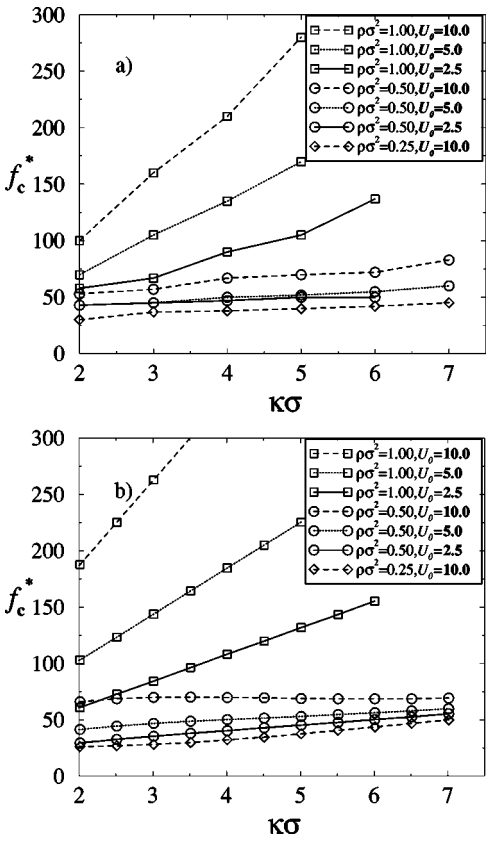

FIG. 5. Critical field strength f_c^* for the two-dimensional system versus $\kappa\sigma$ for different U_0 and $\rho\sigma^2$ as obtained from Brownian dynamics simulation (a) and theory (b). By increasing the field strength f^* the system shows a phase transition from a disordered state to a state characterized by lane formation. The transition is indicated by the symbols, the lines are a guide to the eye.

In Fig. 5(b) we plot the results of our simple theory as described in Sec. IV A for the same parameter combinations as chosen for the simulations in Fig. 5(a). Comparing theory and simulation the theory reproduces all trends correctly. In particular, f_c^* grows with increasing ρ, U_0, and κ as obtained in the simulations. By assigning to α in Eq. (13) a value 2.0 the theory even brings about quantitative agreement, particular for the low density cases ($\rho=0.25, 0.5$) and can thus be used for a simple estimate for the location of the transition towards lane formation. Furthermore, the assumption implicit in our theory that the transition is modified by particle correlations is justified.

Similar results for the nonequilibrium phase transition in *three* spatial dimensions are presented in Fig. 6. We have observed the same trends as in two dimensions. Again the theory is in semiquantitative agreement with our simulation data, though the curvature of the f_c versus $\kappa\sigma$ data is slightly different. Here the optimal fit is $\alpha=1.5$.

B. Oscillating field

For an oscillating external field, data for the critical frequencies ω_c upon which the system goes back into a disor-

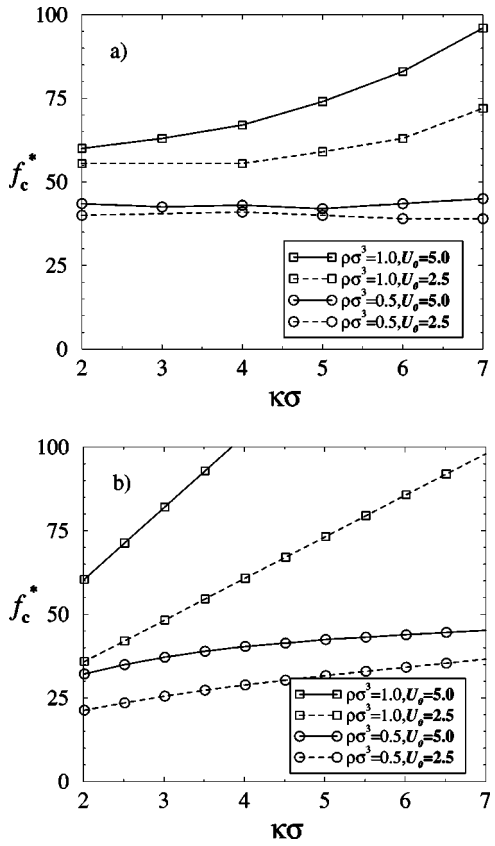

FIG. 6. Same as Fig. 5 for the three-dimensional system: (a) simulation results, (b) theory.

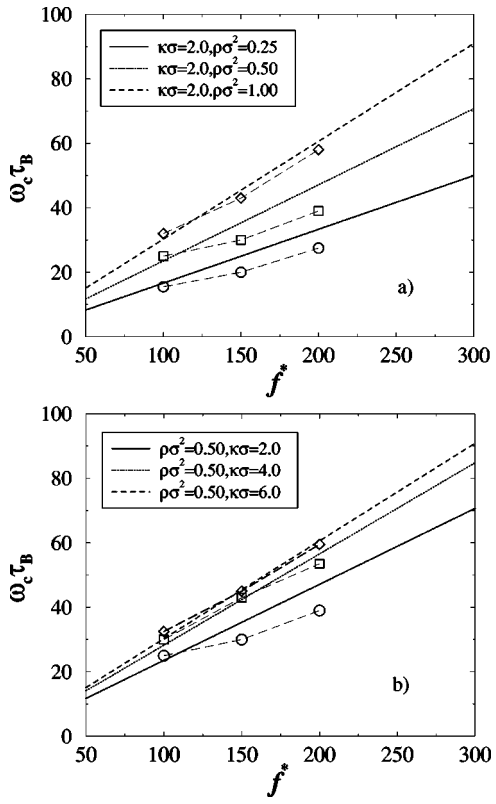

FIG. 7. Nonequilibrium phase diagram for the two-dimensional system with oscillatory external field for $U_0=5.0$. The critical field frequency ω_c in units of $1/\tau_B$ is plotted versus the field amplitude f^* for different densities (a), and for different screening lengths (b). For low frequencies the system stays in the stratified state, while for increasing frequency there is a transition back to disorder. Lines are theoretical estimations, symbols are the corresponding simulation results. The long dashed lines connecting equal symbols are a guide to the eye. In (a) the boundary moves up with increasing density, in (b) the boundary moves up with increasing decay length.

dered state are given in Fig. 7. They are shown versus the field amplitude for different particle densities ρ [Fig. 7(a)] and for different particle interaction ranges $1/\kappa$ [Fig. 7(b)]. The trends are as follows: ω_c increases for increasing amplitude, increasing density, and increasing κ. In our considered parameter range no obvious U_0 dependence was found in the simulation. All these trends are in accordance with our simple theory, which is also plotted in Fig. 7. The theory is even confirmed quantitatively by our simulation data. The discrepancy between theory and simulation is always smaller than 20%, at least in the parameter range where simulations were performed.

VI. CONCLUSIONS

In conclusion we have studied the influence of an external field on a binary colloidal mixture performing Brownian dynamics in a solvent with simulation and simple theory. It was shown that oppositely driven particles avoid each other by forming different lanes due to a nonequilibrium slip-stream effect. Using a suitable order parameter this was identified as a first-order nonequilibrium phase transformation. A simple scaling theory was proposed whose predictions and trends were confirmed by our simulation data. The process of lane formation was found to be very general: it prevails for oscillating fields provided the frequency is not too small and is present both in two and three spatial dimensions. Hence, it should be observable in real systems such as binary colloidal dispersions, e.g., driven by an oscillatory electric field.

It would be very interesting to construct a hydrodynamic theory of pattern formation predicting lane formation as an instability [42,43]. Even more challenging would be a full microscopic nonequilibrium theory, which has been much more elaborated for second-order nonequilibrium phase transitions [6,44].

We finish with a couple of points. First, lane formation is also expected to occur in three-component colloidal systems and, in general, for polydisperse samples. The formation of lanes could provide an efficient channel to transport specific particles into a preferred direction by driving the system via an external field. Second, one might surmise that lane formation will also occur if lattice models other than square lattices are used or if next-nearest-neighbor hopping processes are allowed in the lattice model. This conjecture is based on the observation that shear forces between different lanes are driving the lane formation, which are absent in a square-lattice model with nearest-neighbor hopping. Third, we mention that hydrodynamic interactions [45,46] were neglected

in our study. This is a safe approximation if the colloidal volume fraction is very small as typically realized for highly charged deionized suspensions. As inspired by a recent study of colloidal phase separation [47] we expect that the presence of hydrodynamic interactions will enhance lane formation. Lane formation should also be stable with respect to a change of the particle dynamics. For instance, the transition is expected to be stable also if Fokker-Planck [31] rather than Brownian dynamics is used. The only requirement should be a parallel dynamics for all particles.

ACKNOWLEDGMENTS

We thank R. K. P. Zia, B. Schmittmann, A. Parola, D. Pini, H. K. Janssen, and E. Rebhan for helpful remarks and H. M. Harreis and J. Chakrabarti for useful discussions.

[1] M.P. Allen and D.J. Tildesley, *Computer Simulation of Liquids* (Clarendon Press, Oxford, 1989).
[2] *Observation, Prediction and Simulation of Phase Transitions in Complex Fluids*, Vol. 460 of *NATO Advanced Studies Institute, Series B: Physics*, edited by M. Baus, L.F. Rull, and J.P. Ryckaert (Kluwer Academic, Dordrecht, 1995).
[3] H. Löwen, Phys. Rep. **237**, 249 (1994).
[4] J.P. Hansen and I.R. McDonald, *Theory of Simple Liquids*, 2nd ed. (Academic Press, London, 1986).
[5] S. Katz, J. Lebowitz and H. Spohn, Phys. Rev. B **28**, 1655 (1983).
[6] For a review, see B. Schmittmann and R.K. P.Zia, in *Phase Transitions and Critical Phenomena*, edited by C. Domb and J. Lebowitz (Academic Press, London, 1995) Vol. 17.
[7] J. Marro and R. Dickman, in *Non-equilibrium Phase Transitions in Lattice Models*, edited by C. Godreche (Cambridge University Press, Cambridge, 1999).
[8] S.W. Sides, P.A. Rikvold, and M.A. Novotny, Phys. Rev. Lett. **81**, 834 (1998).
[9] B.K. Chakrabarti and M. Acharyya, Rev. Mod. Phys. **71**, 847 (1999).
[10] R.A. Monetti and E.V. Albano, Physica A **280**, 382 (2000).
[11] M. Aertsens and J. Naudts, J. Stat. Phys. **62**, 609 (1991).
[12] B. Schmittmann, K. Hwang, and R.K.P. Zia, Europhys. Lett. **19**, 19 (1992).
[13] I. Vilfan, B. Schmittmann, and R.K.P. Zia, Phys. Rev. Lett. **73**, 2071 (1994).
[14] T. Mullin, Phys. Rev. Lett. **84**, 4741 (2000).
[15] D. Helbing, I.J. Farkas, and T. Vicsek, Phys. Rev. Lett. **84**, 1240 (2000).
[16] D. Helbing and P. Molnár, Phys. Rev. E **51**, 4282 (1995).
[17] P.N. Pusey, in *Liquids, Freezing and the Glass Transition*, edited by J.P. Hansen, D. Levesque, and J. Zinn-Justin (North-Holland, Amsterdam, 1991).
[18] H. Löwen, Physica A **235**, 129 (1997).
[19] W. Götze, J. Phys.: Condens. Matter **11**, A1 (1999).
[20] For a recent review on colloids in nonequilibrium, see H. Löwen, J. Phys.: Condens. Matter **13**, R415 (2001).
[21] C.A. Murray and D.H. van Winkle, Phys. Rev. Lett. **58**, 1200 (1987).
[22] K. Zahn and G. Maret, Phys. Rev. Lett. **85**, 3656 (2000).
[23] A.H. Marcus, J. Schofield, and S.A. Rice, Phys. Rev. E **60**, 5725 (1999).
[24] H. Löwen, J. Phys.: Condens. Matter **4**, 10 105 (1992).
[25] M.O. Robbins, K. Kremer, and G.S. Grest, J. Chem. Phys. **88**, 3286 (1988).
[26] E.J. Meijer and D. Frenkel, J. Chem. Phys. **94**, 2269 (1991).
[27] M.J. Stevens and M.O. Robbins, J. Chem. Phys. **98**, 2319 (1993).
[28] B. Löhle and R. Klein, Physica A **235**, 224 (1997).
[29] K.J. Naidoo and J. Schnitker, J. Chem. Phys. **100**, 3114 (1994).
[30] H. Löwen and G.P. Hoffmann, Phys. Rev. E **60**, 3009 (1999).
[31] G.P. Hoffmann and H. Löwen, J. Phys.: Condens. Matter **12**, 7359 (2000).
[32] H. Löwen, J.P. Hansen, and J.N. Roux, Phys. Rev. A **44**, 1169 (1991).
[33] D.L. Ermak, J. Chem. Phys. **62**, 4189 (1975); **62**, 4197 (1975).
[34] H. Löwen and G. Szamel, J. Phys.: Condens. Matter **5**, 2295 (1993).
[35] H. Löwen, T. Palberg, and R. Simon, Phys. Rev. Lett. **70**, 1557 (1993).
[36] F. Bitzer, T. Palberg, H. Löwen, R. Simon, and P. Leiderer, Phys. Rev. E **50**, 2821 (1994).
[37] D.M. Heyes and A.C. Branka, Phys. Rev. E **50**, 2377 (1994).
[38] S.R. Rastogi, N.J. Wagner, and S.R. Lustig, J. Chem. Phys. **104**, 9234 (1996).
[39] J. Bergenholtz and N.J. Wagner, Physica A **235**, 34 (1997).
[40] W. Härtl, J. Wagner, C. Beck, F. Gierschner, and R. Hempelmann, J. Phys.: Condens. Matter **12**, A287 (2000).
[41] A.J. Banchio, G. Nägele, and J. Bergenholtz, J. Chem. Phys. **113**, 3381 (2000).
[42] M.C. Cross and P.C. Hohenberg, Rev. Mod. Phys. **65**, 851 (1993).
[43] J. Zhou and M.Z. Podowski, Nucl. Eng. Des. **204**, 129 (2001).
[44] For an example, see K. Oerding and H.K. Janssen, J. Phys. A **28**, 4271 (1995).
[45] G. Nägele, Phys. Rep. **272**, 215 (1996).
[46] J.K.G. Dhont, *An Introduction to Dynamics of Colloids* (Elsevier, Amsterdam, 1996).
[47] H. Tanaka and T. Araki, Phys. Rev. Lett. **85**, 1338 (2000).